Large-scale Integration of Variable Renewables: Higher Temporal Analysis with Optimization Model considering Hydrogen Storage and Rechargeable Battery

Ryoichi Komiyama[a*], Yasumasa Fujii[b]

[a]*Resilience Engineering Research Center, The University of Tokyo, Hongo 7-3-1, Bunkyo-ku, Tokyo 113-8656, Japan*

[b]*Department of nuclear engineering and management, The University of Tokyo, Hongo 7-3-1, Bunkyo-ku, Tokyo 113-8656, Japan*

* Corresponding author. Tel.: +81-03-5841-8970. E-mail address: komiyama@n.t.u-tokyo.ac.jp

Abstract: Although the large-scale integration of VRs (variable renewables) will play a significant role to address energy and environmental issues, it would cause a technical challenge in power grid control. As one of technical countermeasures, hydrogen storage, as well as rechargeable battery, receives growing attention for managing VR intermittency. For adequate renewable energy policy, energy modeling is required to quantify and qualitatively investigate its potential benefits. This paper analyzes the optimal grid integration of large-scale VRs through hydrogen storage and rechargeable battery in Japan with a higher temporal optimal power generation mix model including 100 million constraints. Simulated results reveal that hydrogen storage turns out to be suitable for storing VR energy in a long period of time such as a weekly or monthly scale due to its lower storage loss, while Li-ion battery, NaS battery and pumped-hydro are effective for controlling a shorter cycle variation of VR output. These results suggest that the individual role of those storage technologies should be more elaborately recognized for efficient renewable energy policies to achieve a massive VR integration. Additionally, hydrogen storage installation is promoted by CO_2 regulation policy, suggesting that its implementation enhancing the economic efficiency of hydrogen storage is indispensable.

.

Keyword: Variable renewable, Hydrogen storage, Rechargeable battery, Power generation mix, Optimization

1. Introduction

Large-scale introduction of VRs (variable renewables) such as wind and PV in energy supply has been in the spotlight in order to address energy security and environmental issues. For instance, after Fukushima nuclear accident in Japan, the country has been showing a higher interest in expanding VR energy in its energy mix [1] through the implementation of a Feed in Tariff (FIT) [2], and it is considered as a key option to achieve a limited dependence on nuclear power.

The power outputs of wind and PV, however, inherently hold a large volatility, and the country's power grid control is an important technical challenge for integrating large-scale VRs. Hence, adequate technical measures should be arranged to accomplish an optimal power generation mix integrated with massive VRs. As the technical countermeasures, hydrogen storage system and rechargeable battery are expected to play a key role, besides the curtailment control of surplus VR output. Concerning hydrogen storage combined with VRs, its concept is actually proposed by international manufacturing companies [3,4,5,6,7,8]. In addition, the Japanese government officially announced to support the penetration of the hydrogen produced by renewable energy in the latest national energy plan [1]. The highlight of this research consists in evaluating an optimal policy of installing hydrogen storage and rechargeable battery coupled with VRs in the country's power supply mix.

An economic evaluation of hydrogen storage and rechargeable battery combined with

renewable energy has been performed by employing an energy model in various literatures [9,10,11,12,13,14,15,16,17,18]. However, sufficient studies have not yet been conducted to comprehensively estimate an optimal installation of energy storage technologies such as hydrogen storage, NaS and Li-ion batteries by fully considering VR short-cycle variation in a higher temporal resolution such as a 10-min through a year. The systematic evaluation of VRs in hourly time interval was performed [19], but its analysis in a higher temporal resolution is not sufficiently done so far, and, to the author's knowledge, no study analyzes the nation-wide deployable potential of the battery and hydrogen storage coupled with VRs, considering the short-cycle intermittency of VR output.

So far, the authors developed an optimal power generation mix (OPGM) model, and evaluated a large-scale PV integration in Japan [20] and a potential feasibility of hydrogen storage [21], and the impact of CO2 regulation and nuclear energy policy on the Japanese electric power system [22,23,24]. In this manuscript, for implementing efficient renewable energy policies, the authors develop a higher temporal multi-region OPGM model combined with hydrogen storage and rechargeable battery as a large-scale linear programming model including 100 million constraints and 20 million endogenous variables. This model allows us to assess the optimal deployment and operation of various types of power plants, rechargeable batteries and hydrogen storage in a 10-min resolution through a year, so as to fully take into consideration the VR output intermittency and regional power transmission capacities. By employing this model, this paper attempts to assess an optimal policy for economically integrating large-scale VRs into the Japanese power grid and to provide quantitative insights into the future role of hydrogen storage and rechargeable batteries in the country's power system.

This manuscript is organized as follows: chapter 2 explains the mathematical formulation of a higher temporal multi-region OPGM model; chapter 3 explains calculated results and discusses an economic feasibility of hydrogen storage and rechargeable battery; in chapter 4, major conclusions and implications are explained and future research agenda is suggested.

2. Higher Temporal Multiregional Optimal Power Generation Mix Model

The authors have so far developed an OPGM model for daily load curves in a 10-min resolution through a year under various technical constraints employing a linear programming technique [20][21]. In this paper, the authors furthermore extend the model for considering regional power transmission under the specific tie-line capacity and for combining hydrogen storage with the OPGM model, and analyze its installable potential in the country's power generation mix. The schematic diagram of the developed model is shown in Fig. 1.

In the model developed here, the minimization of a single-period total system cost, including annual facility cost and fuel cost, enables us to specify the optimal mix of power generation and capacity, considering 10-min demand and supply variations on 365 days. The endogenous variable and benchmark cost information is later shown from Table 1 to Table 6, and as later described in Table 7 of section 3, sensitivity analysis on CO2 regulation policy is conducted. One calendar year is decomposed into 52,560 time segments (=6 time points per hour×24 hours per day×365 days per year). Electricity load curve is, however, exogenously given, and demand response, energy saving and load extension measures are not considered. Thus, in this study, the model specifies an optimal mix of power supply technologies under fixed load curve assumption.

This model takes into consideration various power plants as well as energy storage technologies including hydrogen storage. As rechargeable batteries, this paper includes lithium-ion (Li-ion) battery [25] and sodium-sulfur (NaS) battery [26] which performances are distinguished with cost, lifetime

rechargeable cycle, charge and discharge efficiency, and C-rate.

Regarding VR power generation, the model assumes that VR output is supplied to power grid or electrolyzer producing hydrogen, and in some cases, the VR output is curtailed by suppression control as illustrated in Fig. 1. The optimal allocation of VR output for those usages is identified through an optimization. Also, it should be noted that this analysis assumes wind and PV outputs as given variables perfectly predictable in an optimized period and does not consider those uncertainties.

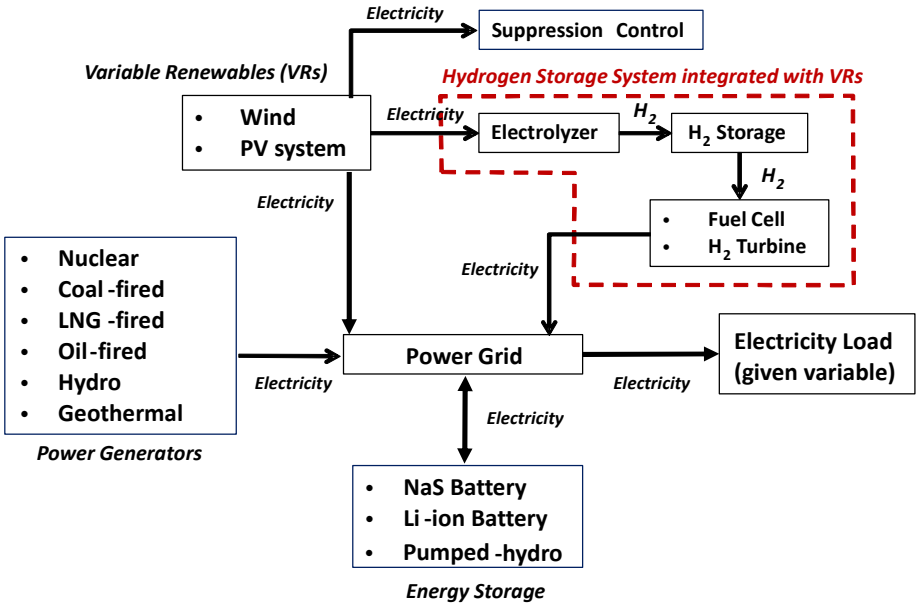

Fig. 1. Schematic diagram of an optimal power generation mix model combined with VR-based hydrogen storage system and rechargeable battery.

As for hydrogen storage system, this paper supposes that an electrolyzer converts surplus VR power output into hydrogen, which is stored in an aboveground compressed steel storage tank and is later converted back into electricity for power grid (Fig.1). The whole amount of the hydrogen produced from VR is assumed to be tentatively stored in the hydrogen storage tank, and the part of the stored hydrogen is used to generate electricity by a stationary fuel cell or a hydrogen combustion turbine if needed. Both technologies are introduced, depending on the assumed costs.

In Japan which has neither major underground salt deposit [27] nor depleted oil and gas deposits, an aboveground compressed tank storage would be a more proper and technically feasible option than an underground storage. Hence, this manuscript only considers the aboveground hydrogen storage. In addition, an electrolyzer is modeled as a centralized electrolysis facility. The system modeled is a standalone electrolyzer based on hydro bipolar alkaline electrolyzer. It uses water for electrolysis. When wind or PV system is closely coupled with the electrolyzer, a direct connection between those VRs and the electrolyzer is possible. This paper assumes that the VRs and the electrolyzer with a hydrogen storage are located close together and the system does not consider the requirement for a long-distance transportation of electricity or hydrogen resulting in a more efficient system.

Regional scope in this paper is the nine regions of nation-wide Japan and the electricity market is assumed as monopoly market. Until now, the authors preliminarily assess the installable potential of VR-based hydrogen system in Tohoku and Hokkaido regions of Japan [21][29] where abundant wind resources, estimated about 70% of the total wind installable potential in Japan [28], are expected.

The highlight of methodology here consists in integrating VR-based hydrogen storage with our

developed multiregional version of the OPGM model [20]. In Ref.[20], the authors develop an optimal power generation mix model and analyze installable PV potential in a detailed temporal resolution. This paper newly combines hydrogen storage with the OPGM model considering regional power transmission topology and evaluates the economic competitiveness of hydrogen storage and rechargeable batteries as power supply options.

Table 1. Endogenous variables in optimal power generation mix (OPGM) model

TC : total annual cost ($/year)
$X_{r,i,d,t}$: output of i-th type of power plants in day d at time t and region r (GW)
$Xin_{u,r,d,t}$: transmitted power from region r to region u in day d at time t (GW)
$Xout_{u,r,d,t}$: transmitted power from region u to region r in day d at time t (GW)
$Xh_{r,i,d,t}$: output of i-th type of power plants (i=PV or Wind) for hydrogen production in day d at time t and region r (GW)
$De_{r,i,d,t}$: Suppressed output of i-th type of power plants (i=PV or Wind) in day d at time t and region r (GW)
$K_{r,i}$: capacity of i-th power plant and region r (GW)
$AvK_{r,i,d}$: available capacity of i-th power plant in day d and region r (GW)
$MtK_{r,i,m}$: unavailable capacity of i-th power plant in m-th maintenance schedule and region r (GW)
$Cha_{r,j,d,t}$: input of j-th electricity storage facility in day d at time t and region r (GW)
$Dis_{r,j,d,t}$: output of j-th electricity storage facility in day d at time t and region r (GW)
$SS_{r,j,d,t}$: stored energy of j-th storage facility in day d at time t and region r (GWh)
$KS1_{r,j}$: kW capacity of j-th electricity storage facility in region r
$KS2_{r,j}$: kWh capacity of j-th electricity storage facility in region r
where. $i \in$ {1: Nuclear, 2: Coal fired, 3: LNGCC, 4: Natural gas fired 5: Oil fired, 6: Hydro, 7: Geothermal, 8: PV, 9: Wind, 10: Fuel Cell, 11: Hydrogen Gas Turbine, 12: Electrolyzer }
$j \in$ {1: Pumped, 2: NaS Battery, 3: Li-ion Battery, 4: Hydrogen Storage Tank}
$d \in \{1, 2, \ldots, D\}$, D : number of the day per year (D=365 or 366)
$t \in \{1, 2, \ldots, T\}$, T : number of the time steps per day (T=24*6=144)
$m \in$ { 1,2,3,4 }
$r, u \in$ {1: Hokkaido, 2: Tohoku, 3: Kanto, 4: Chubu, 5: Hokuriku, 6: Kansai, 7: Chugoku, 8: Shikoku, 9: Kyushu}

This integrated model is formulated through a linear programming technique in a consistent way. The number of the constraints in this model is 100 million, and that of the endogenous variables in Table 1 is 20 million. Employing this developed model, the authors analyze the economic competitiveness of hydrogen storage and rechargeable battery, considering dynamic power system operation in a 10-min through a year. Such a systematic analysis in a high time-resolution has not yet been sufficiently done in any studies before.

The developed model in this paper is expected to support an energy planning for integrating variable renewable with hydrogen storage system and may offer suggestive insight in policy-making concerning the development of sustainable and innovative energy system. However, it should be kept in mind that this paper assumes several hypothesis: perfect predictability of wind and PV variability, perfect control of grid voltage and frequency fluctuations and no requirement of long-distance

hydrogen transportation. Therefore, by paying much attention to the hypothesis influencing the validity of the model, the simulated results need to be understood. Mathematical formulation of the model is described as follows:

2.1 Objective Function

The objective function of the model in equation (1) is composed of annual fixed cost and fuel cost. Fixed costs of elemental facilities is incorporated through the multiplication of capital recovery factor, unit fixed cost ($/kW) and installed capacity (kW). Capital recovery factor is used to annualize initial investment cost.

$$min.\quad TC = \sum_{i=1}^{12}(\mathrm{g}_i \times pf_i \times K_{r,i} + \sum_{r=1}^{9}\sum_{d=1}^{D}\sum_{t=1}^{T} pv_i \times X_{r,i,d,t}) + \sum_{r=1}^{9}\sum_{j=1}^{4} CS_{r,j} \tag{1}$$

$$CS_{r,j} = \left(\mathrm{gs}1_j \cdot psf1_j \cdot KS1_{r,j}\right) + \left(\mathrm{gs}2_j \cdot psf2_j \cdot KS2_{r,j}\right) + (psf3_j \cdot \frac{TCha_{r,j}}{cycle_j}) \tag{2}$$

$$TCha_{r,j} = \sum_{d=1}^{D}\sum_{t=1}^{T} Cha_{r,j,d,t} \tag{3}$$

Where: g_i : annual fixed charge rate of *i*-th type of power plant (capital recovery factor), pf_i : unit fixed cost of *i*-th type of power plants($/kW), pv_i : unit variable cost of *i*-th type of power plants($/kWh), CS_j: annual cost of *j*-th storage facility, $gs1_j$:annual fixed charge rate for power component of *j*-th type of storage facility, $pfs1_j$: unit fixed cost for power component of *j*-th type of storage facility(cost for kW capacity, $/kW), $gs2_j$: annual fixed charge rate for energy component of *j*-th type of storage facility, $pfs2_j$: unit fixed cost for energy component of *j*-th type of storage facility (cost for kWh capacity, $/kWh), $pfs3_j$: unit fixed cost for consumable material, such as electrode, electrolyte and separator of battery technology, of *j*-th type of storage facility($/kWh),$cycle_j$: maximum recharge times of *j*-th type of storage facility, $TCha_j$: annual total charged electricity of *j*-th type of storage facility(kWh/year)

Similarly in the modelling methodology in Ref.[20][21], total cost of rechargeable batteries in equation (2) is decomposed into capital cost proportional to kW capacity (power capacity) including power conditioning system, capital cost proportional to kWh capacity (energy capacity) including battery capital cost, because rechargeable battery cost depends on the power (kW) and energy (kWh) capacity of the system [30,31]. The third term of equation (2) is modelled so that the cost of consumable part such as electrode, electrolyte and separator rises reflecting on the increased number of charge and discharge cycle. As energy storage system, this paper considers NaS battery, Li-ion battery, hydrogen storage and pumped hydro which are suitable to be deployed as large-scale energy storage facilities. And the costs of those technologies are derived from Ref.[32] and Ref.[33], while

other reports provide the relevant cost information [14,31] as well.

2.2 Constraints

(a)Power demand and supply balances

Following balancing constraint is considered so that the power supply from each generator, together with net discharge from rechargeable batteries, is equivalent to the power demand in the region.

$$\sum_{i=1}^{11} X_{r,i,d,t} + \sum_{j=1}^{3} \left(Dis_{r,j,d,t} - Cha_{r,j,d,t}\right) + \sum_{r=1,r\neq u}^{9} in_{u,r} \cdot loss \cdot Xin_{u,r,d,t} - \sum_{r=1,r\neq u}^{9} out_{u,r} \cdot loss \cdot Xout_{u,r,d,t} = load_{r,d,t} \quad (4)$$

$$Xin_{u,r,d,t} = Xout_{r,u,d,t} \qquad (r \neq u) \quad (5)$$

$$Tmax_{u,r} \geq Xin_{u,r,d,t} \quad (6)$$

Where: $load_{r,d,t}$: electric load in day d and region r at time t, *loss*: power transmission loss, $Tmax_{u,r}$: power transmission capacity between region u and region r

(b)Available capacity constraints

Following equations consider that available capacities for power generation are calculated by excluding the capacities under maintenance from total capacities. The maintenance schedule is embedded by considering parameter $ur_{m,d}$, the occurrence rate of plant shutdown in day d due to the maintenance of m-th schedule. This paper assumes the four time profiles of annual maintenance schedule (Fig. 3), considering its seasonal variations.

$$AvK_{r,i,d} + \sum_{m=1}^{4} (ur_{m,d} \cdot MtK_{r,i,m}) = K_{r,i} \quad (i = 1,2,\dots,5,10,\dots,12) \quad (7)$$

$$\sum_{m=1}^{4} (ur_{m,d} \cdot MtK_{r,i,m}) = (1 - upa_i) \cdot K_{r,i} \quad (i = 1,2,\dots,5,10,\dots,12) \quad (8)$$

$$urs_m = \frac{1}{D} \cdot \sum_{d=1}^{D} ur_{m,d} \quad (9)$$

$$\sum_{m=1}^{4} (ur_{m,d} \cdot MtK_{r,i,m}) \geq (1 - upp_i) \cdot K_{r,i} \quad (i = 1,2,\dots,5,10,\dots,12) \quad (10)$$

Where: $ur_{m,d}$: occurrence rate of plant shutdown in day d due to maintenance of m-th schedule [20][21], upa_i : annual average availability of i-th type of power plant, upp_i : seasonal peak availability of i-th type of power plant

(c) Available plant capacity constraints

The power output of each technology must not exceed its maximum available capacity. Concerning wind and PV, the availability factors $uf_{r,I,d,t}$ in equation (13), corresponding to wind and PV output profiles in a 10-min interval through a year as later shown in Fig. 5 and Fig. 6, are exogenously given. These factors are estimated by using the Japanese meteorological database [34] including the 10-min observed information of solar insolation and wind speed. Left-hand side of equation (13) represents the three destinations of output powers from wind and PV. That is, wind and PV outputs are channeled directly into power grid (X), consumed for hydrogen production (Xh) or suppressed (De). The allocations of wind and PV outputs for those usages are determined through the optimization of the model. Equation (14) defines that the power in energy storage facility is charged and discharged under its available kW capacity.

$$X_{r,i,d,t} \leq AvK_{r,i} \quad (i = 1,2,\dots,5,10,\dots,12) \tag{11}$$

$$X_{r,i,d,t} \leq uc_{i,d} \times K_{r,i} \quad (i = 6,7) \tag{12}$$

$$X_{r,i,d,t} + Xh_{r,i,d,t} + De_{r,i,d,t} = uf_{i,d,t} \times K_{r,i} \quad (i = 8,9) \tag{13}$$

$$Cha_{r,j,d,t} + Dis_{r,j,d,t} \leq us1_{j,d} \times KS1_{r,j} \tag{14}$$

$$SS_{r,j,d,t} \leq us2_{j,d} \times KS2_{r,j} \tag{15}$$

Where: $uc_{i,d}$: availability factor of hydro and geothermal power plant, $uf_{r,i,d,t}$: output of unit capacity of PV and wind power plant, $us1_{j,t}$: kW availability factor of j-th type of storage facility, $us2_{j,t}$: kWh availability factor of j-th type of storage facility

(d)Hydrogen energy balances

Equation (16) depicts the input-output energy balance in electrolyzer, where the left hand side represents the product of hydrogen conversion efficiency ($HEFF$) and renewable output (Xh) and the right hand side corresponds to produced hydrogen. Charge and discharge in a hydrogen storage tank is described in equation (17) and (18). Based on hydrogen produced by electrolyzer is charged to the hydrogen storage tank (Cha), and the stored hydrogen is consumed by a fuel cell or a hydrogen gas turbine to generate electricity back into power system.

$$HEFF_{12,d,t} \times \sum_{i=8}^{9} Xh_{r,i,d,t} = X_{r,12,d,t} \tag{16}$$

$$X_{r,12,d,t} = Cha_{r,4,d,t} \tag{17}$$

$$Dis_{r,4,d,t} = \sum_{i=10}^{11} \frac{X_{r,i,d,t}}{HEFF_{i,d,t}} \tag{18}$$

Where: $HEFF_i$: conversion efficiency of hydrogen technology (i=10, 11, 12)

(e)Constraints on upper and lower installable capacity

Installable capacity of considered technology is constrained under its maximum and minimum deployable limitation.

$$K_{r,i} \geq K_{r,0i} \ , \ K_{r,i} \leq K_{r,upper,i} \tag{19}$$

$$KS1_{r,j} \geq KS1_{r,0j} \ , \ KS1_{r,j} \leq KS1_{r,upper,j} \tag{20}$$

$$KS2_{r,j} \geq KS2_{r,0j} \ , \ KS2_{r,j} \leq KS2_{r,upper,j} \tag{21}$$

Where: $K_{r,0i}$, $KS1_{r,0j}$, $KS2_{r,0j}$: existing capacity , $K_{r,upper,i}$, $KS1_{r,upper,j}$, $KS2_{r,upper,j}$: capacity upper limit

(f)Capacity reserve constraint for power supply reliability

A certain level of reserve margin needs to be secured by a following constraint in order to maintain a reliable electricity supply.

$$\sum_{i=1}^{5} AvK_{r,i,d} + \sum_{i=6}^{7} (uc_{i,d} \cdot K_{r,i}) + \sum_{j=1}^{3} (us1_{j,d} \cdot KS_{r,j}) \geq (1+\delta) \times load_{r,d,t} \tag{22}$$

Where: δ : reserve margin (=5~8%).

(g)Constraints on the ramping capability of thermal power plants

Following equations formulate the controllability of electric power output in each power plant. Each type of power plant has its own capability of ramping up and down due to the technical characteristics, and the power generation of each plant can be adjusted within its output controllability. Ref.[20] provides the more detailed explanations. Those features are formulated as follows.

$$X_{r,i,d,t+1} \leq X_{r,i,d,t} + increase_i \times \{(1-\lambda_i)X_{r,i,d,t} + \lambda_i \cdot AvK_{r,i,d}\} \quad (i = 1,2,\dots,5,10,11,12) \tag{23}$$

$$X_{r,i,d,t+1} \geq X_{r,i,d,t} - decrease_i \times \{(1-\lambda_i)X_{r,i,d,t} + \lambda_i \cdot AvK_{r,i,d}\} \quad (i = 1,2,\dots,5,10,11,12) \tag{24}$$

$$X_{r,i,d,t+1} \leq X_{r,i,d,t} + increase_i \times \{(1-\lambda_i)X_{r,i,d,t} + \lambda_i \cdot uc_{i,d,t} \cdot X_{r,i,d,t}\} \quad (i = 6,7) \tag{25}$$

$$X_{r,i,d,t+1} \geq X_{r,i,d,t} - decrease_i \times \{(1-\lambda_i)X_{r,i,d,t} + \lambda_i \cdot uc_{i,d,t} \cdot X_{r,i,d,t}\} \quad (i = 6,7) \tag{26}$$

Where: $increase_i$: maximum output increase rate per unit time of i-th type power plant, $decrease_i$: maximum output decrease rate per unit time of i-th type power plant, λ_i: capacity weight in the present output level (=0.5 for default setting in this study).

(h)Minimum output constraint on thermal power plants

Equation (27) explains that a thermal power plant can generate electricity at more than its minimum output threshold, excluding the thermal plant served as DSS (Daily Start and Stop) generator (*dss*) [20]. A thermal power plant with DSS mode produces electricity under quick heat-up and cool-down cycle for rapid demand increase and decrease, and that without DSS mode, on the other hand, operates at more than its minimum output level, based on equation (27). The right-hand side value of equation (27), which is a multiplication of available plant's capacity without DSS mode (*Dmax-dss*AvK*) and a ratio of minimum output level (*mol*), corresponds to the plant's minimum output level without DSS mode. These equations from (27) to (29) are only applicable to LNGCC, LNG and oil-fired power plant. Maximum output level (*DMax*) of the plant, included in the right-hand side of equation (27), is estimated through equation (28) and (29).

$$X_{r,i,d,t} \geq (DMax_{r,i,d} - dss_i \cdot AvK_{r,i,d}) \cdot mol_i \tag{27}$$

$$DMax_{r,i,d} \geq X_{r,i,d,t} \tag{28}$$

$$DMax_{r,i,d} \geq X_{r,i,d+1,t} \tag{29}$$

Where: $DMax_{r,i,d}$: maximum output level of i-type power plant in day d and d+1, dss_i: share of daily start and stop operation (DSS) of i-type power plant, mol_i: minimum output level ratio of operation of i-th type power plant

(i)Charge and discharge balances of energy storage technologies

State equation (30) explains energy charge (*Cha*) and discharge (*Dis*) balances for stored energy (*SS*) in each storage facility. The energy balances in hydrogen storage tank, as well as NaS, Li-ion battery and pumped hydro, are described by following equation.

$$SS_{r,j,d,t+1} = \left(1 - sd_j\right) \cdot SS_{r,j,d,t} + \left(\sqrt{eff_{storage,j}} \cdot Cha_{r,j,d,t} - \frac{1}{\sqrt{eff_{storage,j}}} \cdot Dis_{r,j,d,t}\right) \cdot Tw \tag{30}$$

Where: sd_j: Self discharge rate, $eff_{storage}$: Cycle efficiency of electricity storage, Tw : step width of the unit time (10-min)

(j)Available capacity constraint of energy storage technology

Total stored electricity in power storage technology is constrained by its available storage capacity according to equation (31).

$$SS_{r,j,d,t} \leq m_{storage,j} \times u_{j,d} \times KS1_{r,j} \tag{31}$$

$m_{storage}$: Energy storage capacity per generation capacity,

(k)C-rate constraints of rechargeable battery technologies

Charged or discharged electric power is restricted depending on the C-rate of each rechargeable battery such as NaS and Li-ion. The model in this paper considers those technical performances of each battery technology by following constraints.

$$Cha_{r,j,d,t} \leq C-rate_j \times KS2_{r,j} \quad (j = 2,3) \tag{32}$$

$$Dis_{r,j,d,t} \leq C-rate_j \times KS2_{r,j} \quad (j = 2,3) \tag{33}$$

Where: $C\text{-}rate_j$: C-rate of type j of battery technology

(l)CO_2 emissions constraint

$$\sum_{i=2}^{5}(carbon_i \times \sum_{r=1}^{9}\sum_{d=1}^{D}\sum_{t=1}^{T} X_{r,i,d,t}) \cdot Tw \leq co2_{upper} \tag{34}$$

Where: $carbon_i$: Carbon intensity of fuel of i-th type power plant, $co2_{upper}$: Annual CO_2 emissions limit

2.3 Input data

(a) Estimated PV Output

The annual profile of the nation-wide PV output in Japan is estimated by using a numerical solar irradiance model, as described in Ref.[20], with AMeDAS (Automated Meteorological Data Acquisition System) observation database [34]. The database incorporates the 10-min data of sunshine duration, precipitation and ambient temperature. The regional average PV output is assessed by the arithmetic average of the estimated PV outputs at almost all of AMeDAS observation sites in each region of Japan. The estimated PV output of unit capacity in the region during the year 2007 is shown in Fig. 2. The figure implies that the intensity of solar insolation shows a higher level in summer and a lower level in winter season. Therefore, if PV holds a large fraction in the power grid for the future, solving the seasonal imbalance of PV output will become a key agenda.

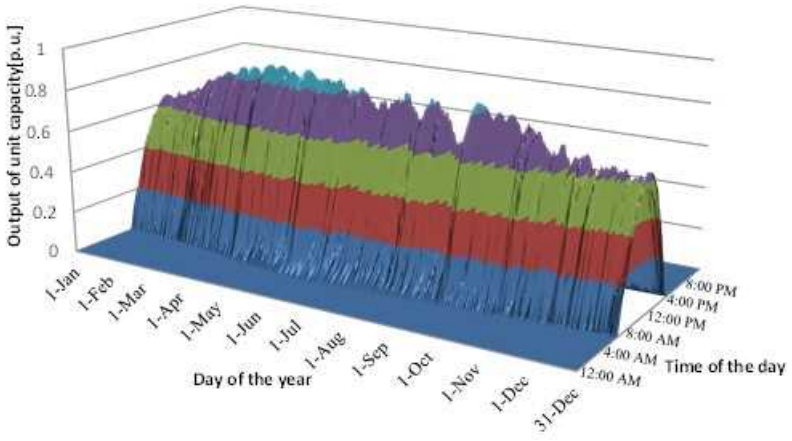

(a) Kanto

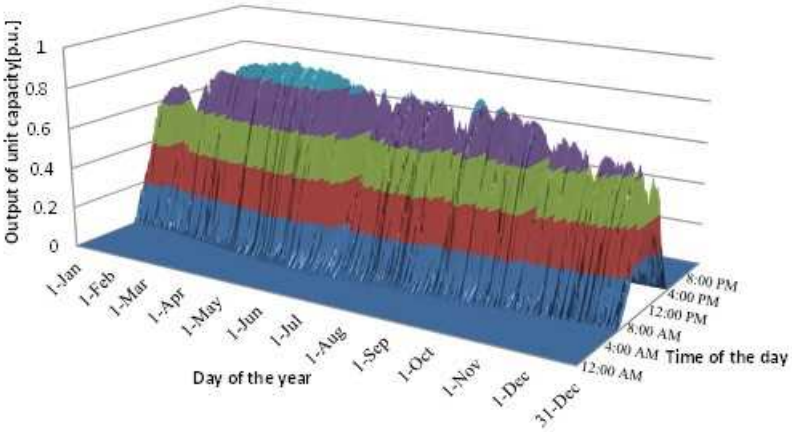

(b) Kansai

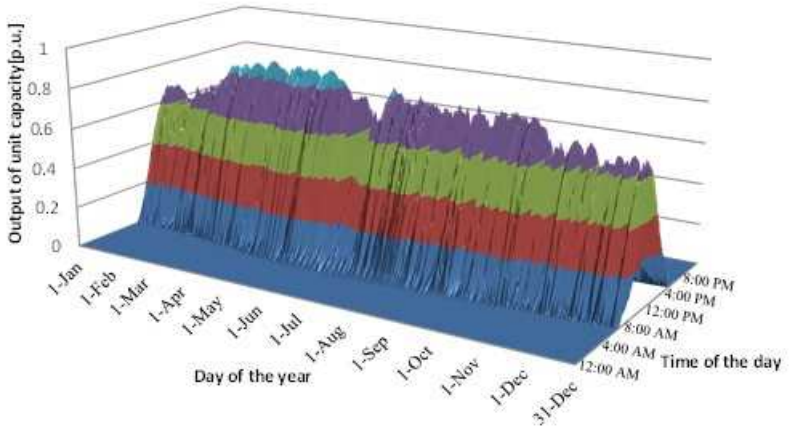

(c) Kyushu

Fig.2. PV output profile in each region of Japan (2007). Horizontal axis indicates the day of the year (365 days), and normal axis, time of the day in a 10-min resolution.

(b) Estimated Wind Power Output

The authors assessed a nation-wide wind output in Japan at a 10-min interval from the AMeDAS observation database. The estimation flow of wind output at each observation site in the region is described in Ref.[20]. The estimated wind output of unit capacity during the year 2007 is shown in Fig. 3. It turned out that there is significant seasonal variation in the wind output profile of Tohoku, with a higher intensity in winter and spring seasons and a lower intensity in summer season.

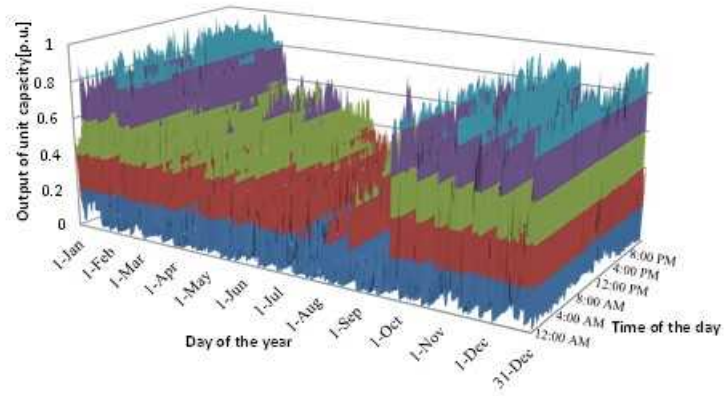

(a) Hokkaido

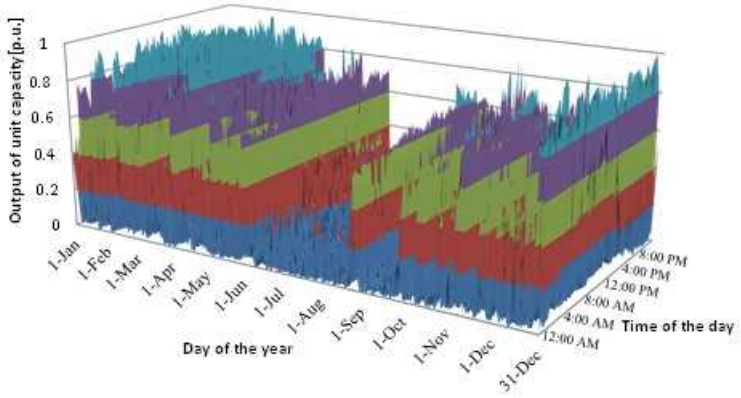

(b) Tohoku

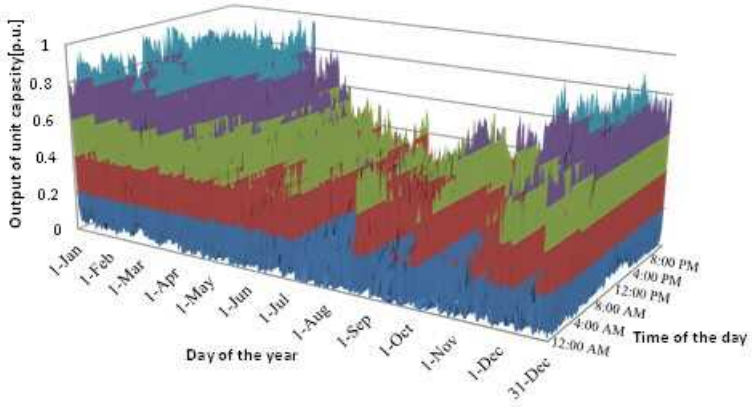

(c) Kyushu

Fig.3. Wind output profile in each region of Japan (2007). Horizontal axis indicates the day of the year (365 days), and normal axis, time of the day in a 10-min resolution.

(c)Regional transmission capacity in Japan

In addition, this paper explicitly considers upper limits of inter-regional tie line capacities as shown in Fig.4. The values of capacities are exogenously given according to the data compiled by Electric Power System Council of Japan.

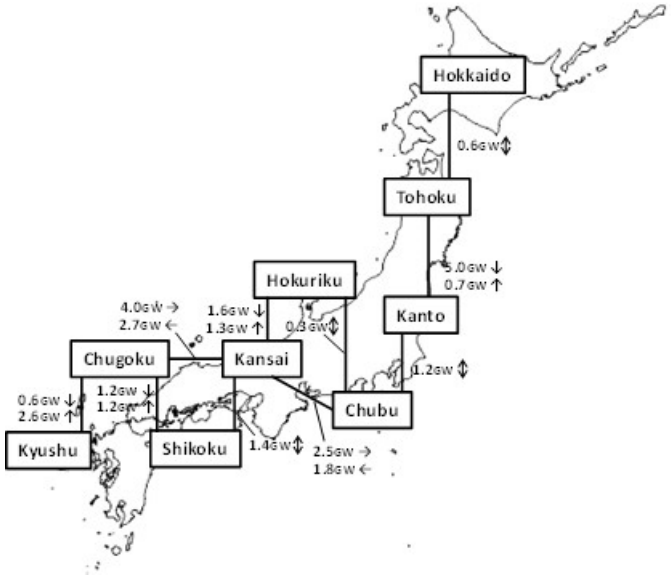

Fig. 4. Upper limit capacities of regional power interchanges in Japan

2.4 Other Exogenous Parameters for OPGM Model

Table 2, Table 3, Table 4, Table 5 and Table 6 show the assumed parameter values of the optimal power generation mix model. The exogenous variables besides hydrogen technologies are based on Ref.[20]. Source data of hydrogen storage, hydrogen-fueled power generation and electrolyzer are derived from the publicly available literatures [11,12,14,15,35] and is regarded as the benchmark of the calculation. As later described in Table 7 of section 3, the calculation is conducted based on this benchmark cost and lower cost.

Table 2. Input data for nuclear and thermal power plant

Type	Nuclear	Coal	LNG GCC	LNG ST	Oil
Unit Construction Cost [$/kW]	2790	2300	1200	1200	1900
Life Time [year]	40	40	40	40	40
Annual O&M Cost Rate	0.04	0.048	0.036	0.036	0.039
Maximum Capacity [GW]	3.27	3.55	∞	∞	∞
Minimum Capacity [GW]			2.70	3.00	1.98
Efficiency	1.00	0.42	0.48	0.40	0.39
Own Consumption Rate	0.04	0.06	0.02	0.04	0.05
Fuel Cost [Yen/specific unit]	1.67	7.45	43.12	43.12	46.66
Heat Content[kcal/specific unit]	860	6139	13043	13043	9126
Carbon Content[kg-C/specific unit]	0.00	0.62	0.75	0.75	0.79
Maximum Increase Rate of Output	0.00	0.31	0.82	0.82	1.00
Maximum Decrease Rate of Output	0.00	0.58	0.75	0.75	1.00
Capacity Weight in Present Output Level (λ)	0.50	0.50	0.50	0.50	0.50
Seasonal Peak Availability	0.85	0.85	0.90	0.90	0.90
Annual Average Availability	0.85	0.78	0.83	0.80	0.80
Share of Daily Start and Stop (dss)	0.00	0.00	0.50	0.30	0.70
Minimum Output Level (mol)	0.30	0.30	0.20	0.20	0.30
Specific Unit	kWh	kg	kg	kg	l

Table 3. Input data for hydro and geothermal

Type	Hydro	Geothermal
Unit Construction Cost [$/kW]	8500	8000
Life Time [year]	60	50
Annual O&M Cost Rate	0.0178	0.01
Maximum Capacity [GW]	1.95	0.22
Minimum Capacity [GW]		
Maximum Increase Rate of Output	0.05	0.05
Maximum Decrease Rate of Output	0.05	0.05
Capacity Weight in Present Ouput Level	0.5	0.5

Table 4. Input data for PV and wind

Type	PV	Wind
Unit Construction Cost [$/kW]	6000	1770
Life Time [year]	20	20
Annual O&M Cost Rate	0.01	0.02
Maximum Capacity [GW]	∞	∞
Minimum Capacity [GW]	0	0

Table 5. Input data for pumped-hydro and rechargeable battery

Type	Pumped	NaS	Li-ion
Unit kW Construction Cost [$/kW]	2400	1200	1000
Life Time [year]	60	15	10
Annual O&M Cost Rate	0.01	0.01	0.01
Maximum Capacity [GW]	0.462	∞	∞
Minimum Capacity [GW]		0	0
Unit kWh Construction Cost [$/kWh]	10	40	200
Annual O&M Cost Rate	0.01	0.01	0.01
Maximum Capacity [GWh]	2.772	∞	∞
Minimum Capacity [GWh]		0	0
Unit Non durable Material Cost [$/kWh]	0	160	800
Life Cycle [times]	-	4500	3500
Cycle Efficiency	0.70	0.90	0.95
Self Discharge Loss [1/hour]	0.0001	0.001	0.001
Maximum kWh ratio to kW	6	∞	∞
C Rate	-	0.14	2.00

Table 6. Input data for hydrogen storage tank

Type	Hydrogen
Unit kW Construction Cost [$kW]	702
Life Time [year]	15
Annual O&M Cost Rate	0.01
Maximum Capacity [GW]	∞
Minimum Capacity [GW]	0
Unit kWh Construction Cost [$/kWh]	15
Annual O&M Cost Rate	0.01
Maximum Capacity [GWh]	∞
Minimum Capacity [GWh]	0
Unit Non durable Material Cost [$/kWh]	0
Life Cycle [times]	∞
Cycle Efficiency	0.90
Self Discharge Loss [1/hour]	0.0001
Maximum kWh ratio to kW	∞

3. Results and discussions

Employing the OPGM model in Fig. 1, this study estimates the installable potential of energy storage technologies including the hydrogen storage system which utilizes surplus VR output for producing and storing hydrogen together with rechargeable battery, and attempts to identify the potential economic barriers for achieving a sustainable energy system. The authors perform a sensitivity analysis to evaluate the economic competitiveness of hydrogen produced from VRs via electrolysis with hydrogen storage. The sensitivity study is mainly conducted on following two items: CO_2 regulation policy and the cost of hydrogen storage system. Table 7 shows the numerical

information assigned in this sensitivity analysis.

Table 7. Case settings regarding CO_2 regulation and hydrogen system cost

Reduction ratio of CO_2 emissions	No regulation, 50%, 80%
Reduction ratio of hydrogen system cost	0%, 25%, 50%, 60%, 70%, 80%, 90%

CO_2 emissions are regulated by the indicated ratio in Table 7 as well from the level of the emissions without the regulation. Regarding the hydrogen system cost, the costs of all elemental technologies including electrolyzer, hydrogen storage and hydrogen-fueled power generator are assumed to be declined together by the designated ratio in Table 7.

Based on calculated results according to all the case settings in Table 7, hydrogen storage is observed to be introduced when its cost is considerably declined. Hence, in this chapter, the results are mainly shown in the case where the cost of the hydrogen storage system is decreased by 90%.

3.1 Optimal Mix of Power Generation and Capacity

Power generation mix and capacity mix are illustrated respectively in Fig. 5 and Fig. 6 under each case of CO_2 regulation. Additionally, those figures are estimated on the basis of the assumption that the costs of all the hydrogen storage components (electrolyzer, storage tank and hydrogen generator) are reduced by 90% from the reference cost.

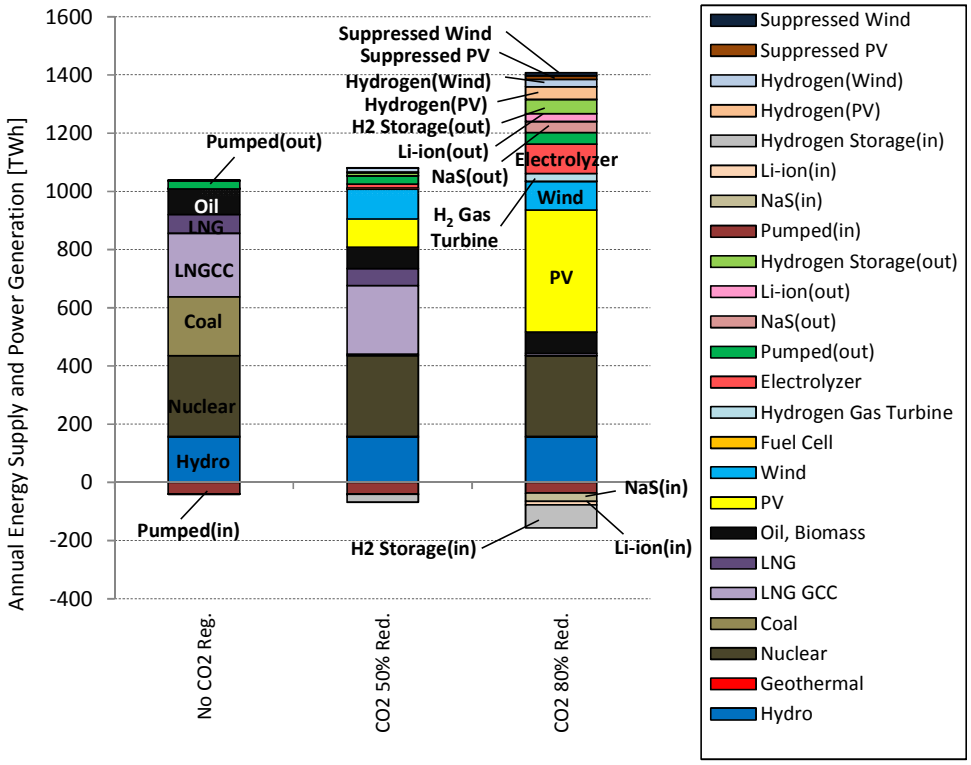

Fig.5. Power generation of each technology under individual CO_2 regulation policy in Japan (hydrogen storage system cost: 90% reduction).

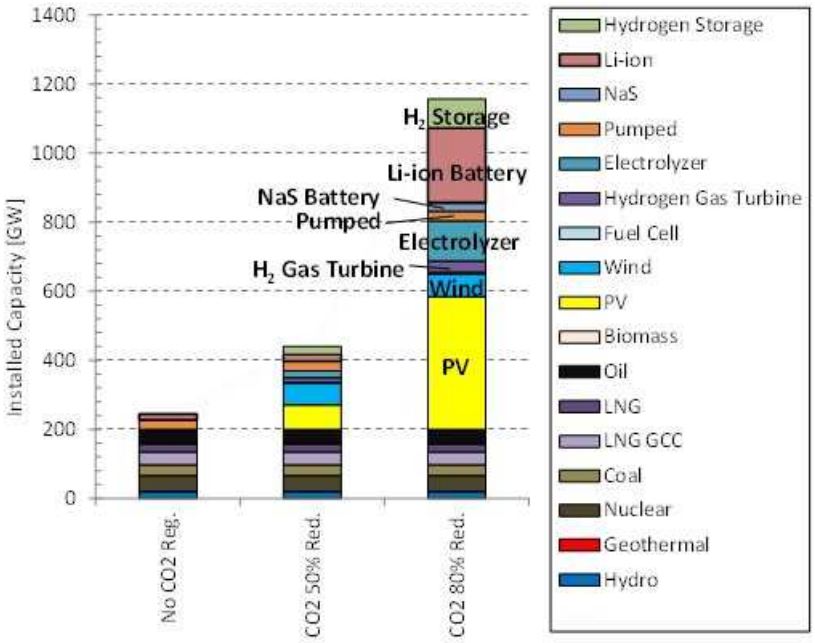

Fig.6. Installed capacity of technologies under individual CO_2 regulation policy in Japan (hydrogen storage system cost: 90% reduction).

In this paper, it should be noted that the installed capacities of nuclear power, coal-fired, oil-fired, hydro, pumped storage are fixed at the present values.

Fig. 5 and Fig. 6 suggest that strict CO_2 regulation policy accelerates the installation of PV, wind power and energy storage system, such as hydrogen storage, Li-ion battery and NaS battery. These technologies alternatively replace carbon-intensive thermal power plants such as coal and natural gas-fired power plants. In Japan, wind power has a higher usage ratio than PV as shown in Fig. 2 and Fig. 3, and wind power has more economic advantage compared with PV. However, as already described, wind resources are concentrated on northern part of Japan (Hokkaido, Tohoku) and maximum limit of tie-line capacity in those regions become bottleneck to expand wind in the country's energy mix. By contrast, PV power, which resources are available nationwide in Japan and has no constraints associated with regional tie-line capacity, shows a significant growth under strict CO2 regulation policy. Regarding energy storage technologies, as depicted in Fig. 6, the capacities of hydrogen storage and rechargeable battery tend to increase in conjunction with the extensive introduction of PV and wind. Stored hydrogen is chiefly supplied to the hydrogen gas turbine which has better economic performance than fuel cell.

Based on Fig. 5, Fig. 7 shows the breakdown of PV and wind power output, which is composed of those outputs into power grid, into hydrogen production and its output suppression control. In the case of CO_2 80% reduction, 20% of wind output and 10% of PV output are used for hydrogen production, while 10% of wind output and 3% of PV output is curtailed.

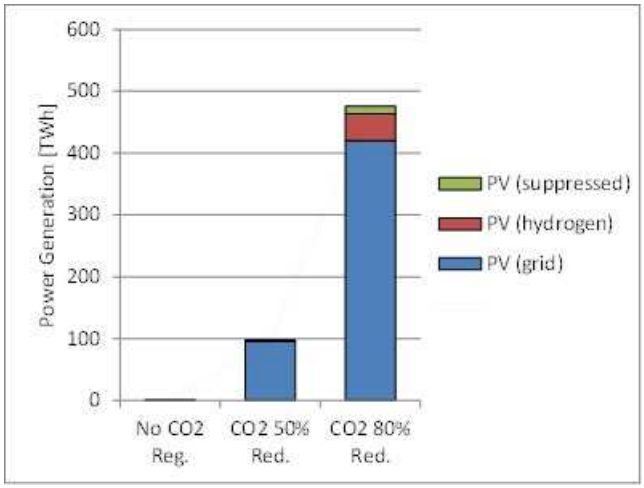

(a) PV

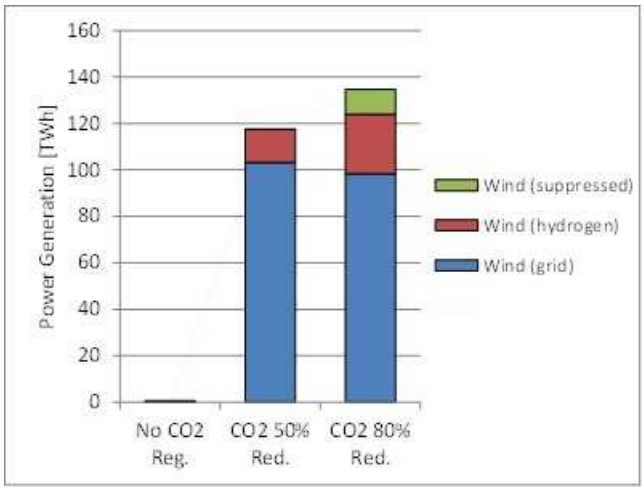

(b) Wind

Fig.7. Breakdown of PV and wind power outputs into power grid, hydrogen production and its suppression (hydrogen storage system cost: 90% reduction). This breakdown is endogenously determined by the model through an optimization.

3.2 Power Generation Dispatch

Fig. 8 depict the simulated monthly optimal dispatches of power generators on January in Japan at individual CO_2 regulation policy where 90% cost reduction of hydrogen storage is assumed. The fraction of wind in total annual power generation in Fig. 8(b) and Fig. 8(c) is both 10%, while the ratio of PV in Fig. 8(b) and Fig. 8(c) is 10% and 40% respectively. Thus, PV holds the largest share in power generation mix at CO2 80% reduction policy. As already illustrated in Fig. 3, there are considerable seasonal variations in the wind output profile in Japan; wind output shows a higher intensity in winter and spring seasons and a lower intensity in summer season. Therefore, Fig.8 (January) shows the result where higher wind output is occasionally observed through a year.

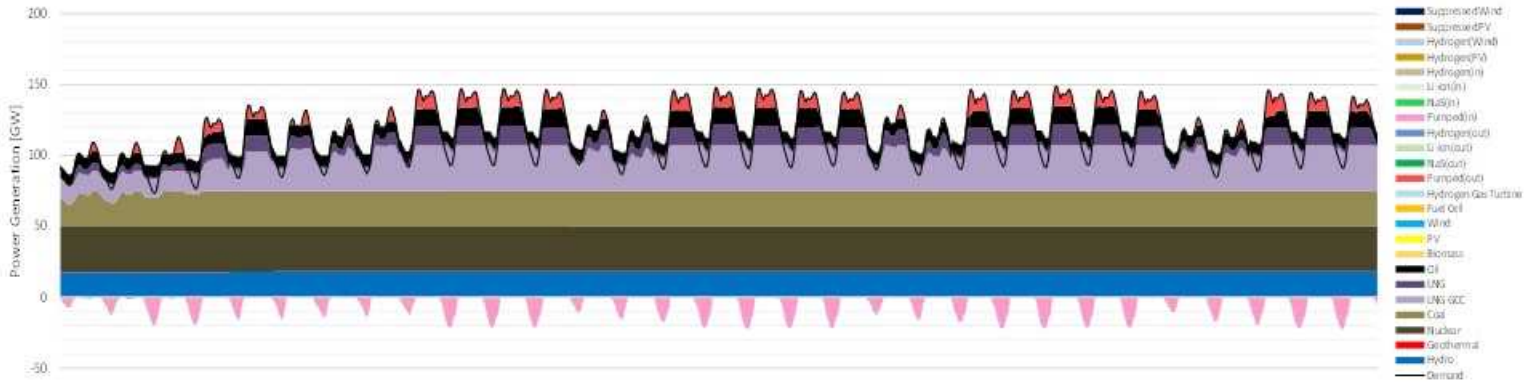

(a)No CO_2 regulation

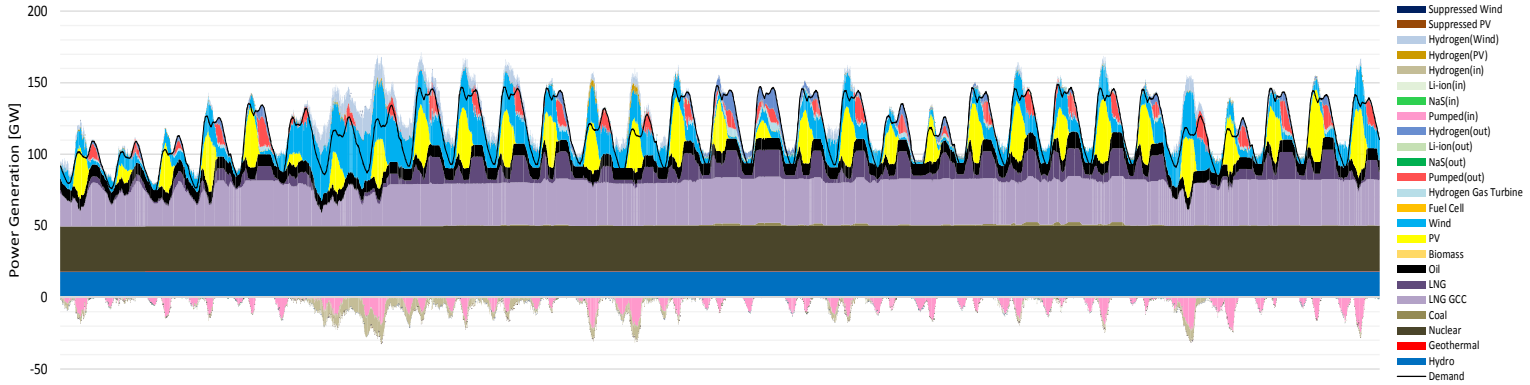

(b)CO_2 50% reduction

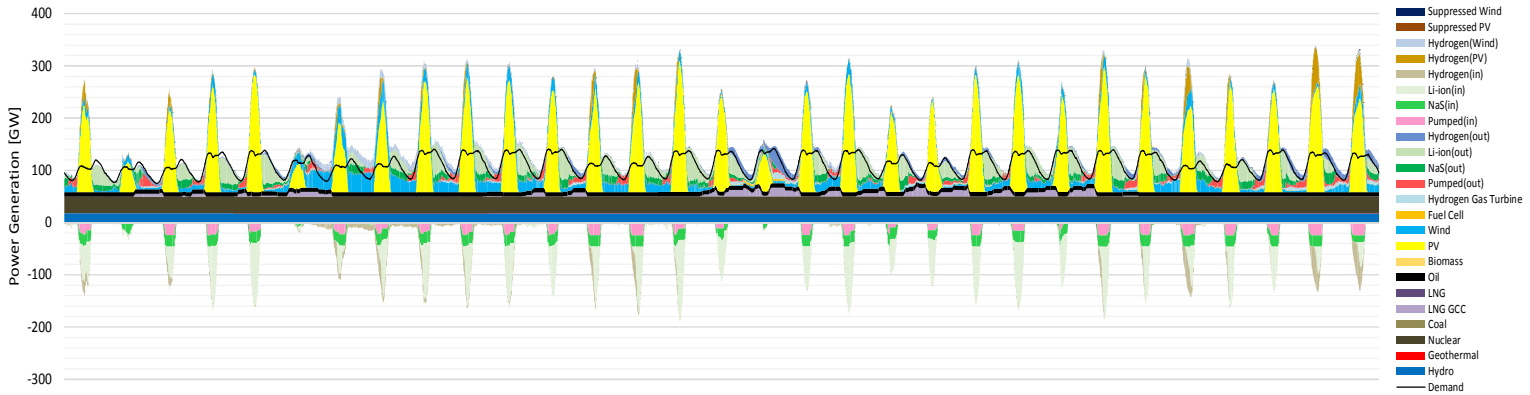

(c)CO_2 80% reduction

Fig.8. Monthly power generation profile of Japan in January under individual CO_2 regulation policy (hydrogen storage system cost: 90% reduction).

According to Fig. 8(b) (CO_2 50% reduction), in January where good wind condition is observed and the wind power is frequently dominant in total power generation mix, a part of excessive wind output is converted into hydrogen and stored into a compressed hydrogen tank. Based on Fig. 8(c) (CO_2 80% reduction) where PV become dominant in power generation mix due to the limited wind expansion caused by power transmission bottleneck, surplus PV output is transformed into hydrogen and stored in hydrogen tank as well In the time periods when PV and wind output sometimes becomes lower in January, a hydrogen combustion turbine consuming compressed hydrogen of the tank complementally provides a power supply in the grid.

3.3 Stored Energy Balance in Hydrogen Storage and Rechargeable Battery

Fig. 9 shows the yearly profile of stored energy in energy storage technologies such as hydrogen storage tank, NaS and Li-ion batteries and pumped storage under each CO2 regulation.

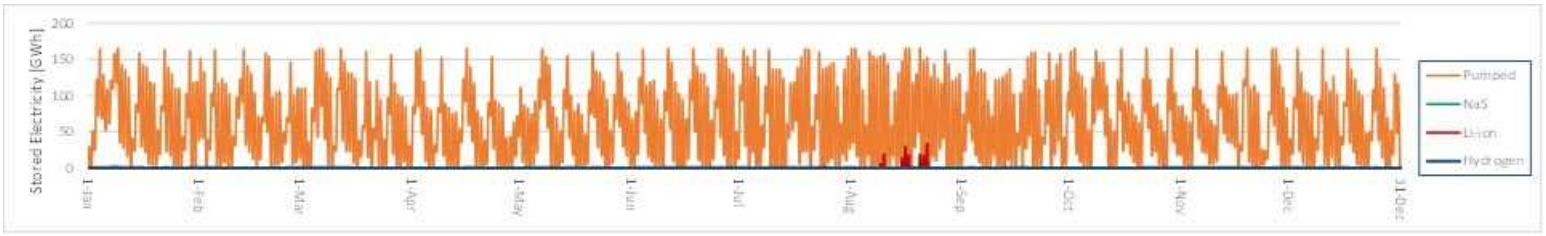

(a) No CO_2 regulation

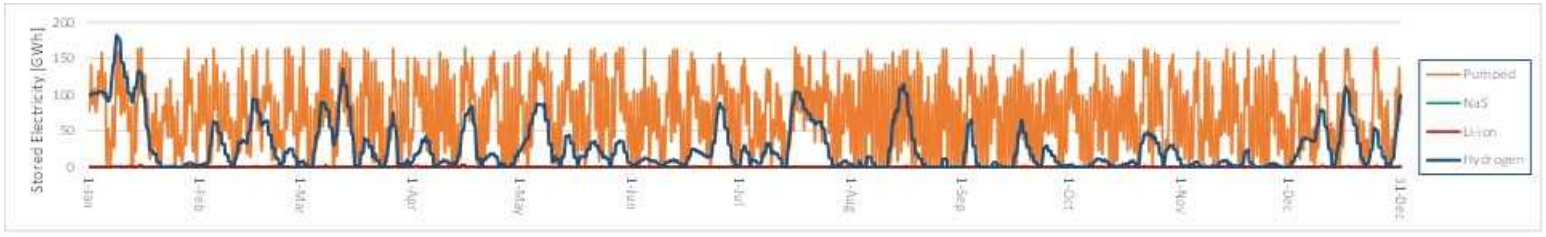

(b)CO_2 50% reduction

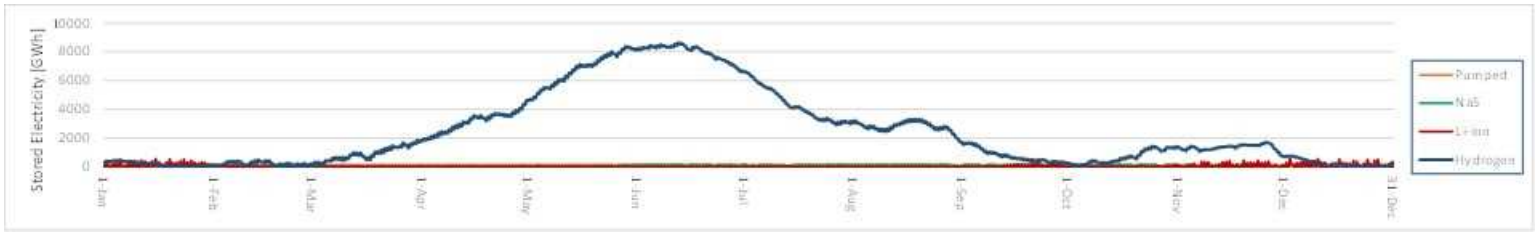

(c) CO_2 80% reduction (all storage technologies)

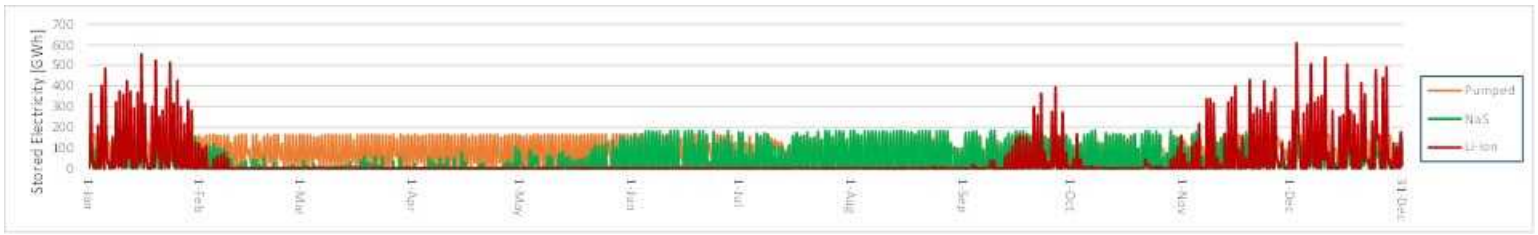

(d) CO_2 80% reduction (Pumped, NaS and Li-ion)

Fig.9. Yearly 10-min profile of stored energy in energy storage technologies under individual CO_2 regulation policy. Horizontal axis indicates the day of the year (365 days in 10-min), and vertical axis, stored energy in energy storage technology (hydrogen storage system cost: 90% reduction).

In Fig.9(a) where the penetration of VR energy is marginal, only pumped-hydro storage, conventional storage technology, is introduced to achieve an economical power demand and supply balance. In Fig.9(b) where VR energy accounts for 20% of total power generation mix, together with pumped-hydro, hydrogen storage play an important role to treat an excessive output of PV and wind power, and most hydrogen energy is stored in a compressed hydrogen tank in a weekly scale. And in Fig.9(c) where VR energy explains 50% of total power generation, from March to May when wind and PV output intensity is higher and those sufficient outputs are available, a lot of hydrogen is produced by those surplus outputs and a large amount of hydrogen energy is stored in a hydrogen tank for a long-term interval such as a monthly scale (Fig.9(c)). Since a storage loss of hydrogen in the compressed tank is very low, the developed energy model selects a long-term hydrogen storage of surplus VR output as an optimal solution under strict CO_2 regulation. Additionally, based on Fig.9(d) which more focusing the operational behavior of storage technologies excluding hydrogen tank, Li-ion battery turns out to be effective for controlling a short-period variation of wind output which intensity becomes stronger from September to February. Li-ion battery shows higher C-rate and it can treat the short-cycle variation of wind output, in particular. Under this stringent CO_2 regulation policy (Fig.9(d)), pumped-hydro and NaS battery are also installed and adjust the short-cycle variation of power balance as well (Fig.9(d)). These results suggest that the individual role of those storage technologies should be more elaborately recognized for efficient renewable energy policies to accomplish a large-scale VR integration. Thus, the hydrogen storage is a suitable option for storing excessive VR output in a weekly or monthly scale as represented by Fig. 9.

4. Conclusions and Implications

For the better formation of the country's renewable energy policies, hydrogen storage system coupled with VRs is a viable option to produce environmentally-benign hydrogen, being promised to effectively integrate a larger fraction of VR energy into the power grid. If that VR-based hydrogen storage becomes economically competitive enough to be penetrated in the market for the future, it can be a sustainable pathway for efficiently using VR energy to reduce a dependence on fossil fuels and mitigate CO_2 emissions. And recently, accelerated VR deployment shows a potential sign of tackling challenges for the grid management in Japan. Although rechargeable battery has been chiefly investigated as a technical option for integrating large-scale VRs into power system, hydrogen storage could provide additional economic and environmental advantages as well. In order to realize the effective penetration and use of hydrogen energy produced by VRs, it is important to quantify and qualitatively understand its potential benefits and impacts.

Against those backgrounds, this study develops an optimal power generation mix model considering hydrogen storage and rechargeable battery to analyze its cost competitiveness in Japan under numerous possible assumptions of CO_2 regulation policy. Estimated results from this study are expected to support researchers and policy-makers determine where energy-planning efforts should be highlighted if VRs such as wind power are to play a central role in the future power system.

Calculated results suggest that the economic rationality of VR-based hydrogen storage system is enhanced by CO_2 regulation policy, promoting its installation in the country's power generation mix (Fig.5, Fig.6 and Fig.8). Since the hydrogen storage has double energy conversion loss consisting of the loss in water electrolysis converting VR output to hydrogen and that in hydrogen-fueled generator converting hydrogen to electricity into power grid, it needs to improve its economic performance enough to be integrated in power system. In this sense, the implementation of carbon regulation policy which upgrades the economic efficiency of hydrogen storage is indispensable. The cost of hydrogen

technologies should be more elaborately recognized for the formulation of effective energy policies to integrate large-scale VRs in an economical manner.

The results reveal as well that the hydrogen storage of VR output in a long-term interval such as a weekly or a monthly scale becomes an optimal solution (Fig.9(c)), because the energy storage loss of compressed hydrogen storage tank is sufficiently small to economically justify the long-term energy storage. In terms of planning effective renewable energy policies, hydrogen storage is considered to be a suitable option for storing VR energy for a long period of time. By contrast, Li-ion battery is effective for controlling a short-cycle variation of wind output (Fig.9(d)). Pumped-hydro and NaS battery are also installed and adjust the short-cycle variation of power balance as well (Fig.9(d)). These results suggest that the individual role of both technologies should be more elaborately recognized for efficient renewable energy policies to achieve a large-scale VR integration.

The use of hydrogen energy from surplus VR output for energy storage provides a unique opportunity for achieving massive VR integration. In the regions of high electricity transmission congestion or remote locations currently without transmission lines, hydrogen usage may potentially prove more economical than the expansion of electric power grid. Therefore, as future agenda to be investigated, it is important to develop the model considering both the network topology of electricity transmission grid and the geographical distribution of renewable resource in a more detailed way. The consideration of end-use hydrogen technologies such as fuel cell vehicle and end-use stationary fuel cell is important research agenda as well. Furthermore, considering demand response behavior and demand extension resources such as electricity heat-pump water heater and electric vehicle are regarded as future works.

Reference

[1] Ministry of Economy, Trading and Industry, Japan (METI). Establishment of the Strategic Energy Plan of Japan. METI; 2014 Apr. (in Japanese)
Available from: http://www.meti.go.jp/press/2014/04/20140411001/20140411001-1.pdf.

[2] Ministry of Economy, Trading and Industry, Japan (METI). Basic document of calculating procurement price for FIT. METI; 2013 Jan. (in Japanese)
Available from http://www.meti.go.jp/committee/chotatsu_kakaku/pdf/010_s02_00.pdf.

[3] Watanabe H, Kameda T, Yamada M. Hydrogen electric power storage system using renewable electricity. TOSHIBA review 2013;68(7):35-38.(in Japanese)

[4] Siemens AG [Internet]. SILYZER: A Proton-Exchange-Membran-Technology (PEM) based on Electrolysis System; c2006-2014 [cited 2014 May 21]. Available from
http://www.industry.siemens.com/topics/global/en/pem-electrolyzer/silyzer/Pages/silyzer.aspx.

[5] Siemens AG. Second Wind for Hydrogen. Pictures of the Future. 2011 Spring. Available from
http://www.siemens.com/innovation/apps/pof_microsite/_pof-spring-2011/_pdf/pof_0111_strom_electrolysis_en.pdf.

[6] Siemens AG. The Most Versatile Fuel. Pictures of the Future. 2012 Spring. Available from

http://www.siemens.com/innovation/apps/pof_microsite/_pof-spring-2012/_pdf/45_en.pdf

[7] Siemens AG. Integration of Regenerative Energy into Power2Gas by PEM Electrolyzer Technology
-CO2RRECT Project. Smart Grid-Infotage 2013; 2013 Nov 6; München, Germany. Available from http://www.industry.siemens.com/topics/global/en/pem-electrolyzer/silyzer/Documents/2013-11-06_SMARTGRID_Munich_stick.pdf.

[8] Waidhas M. Potential and Challenges of PEM Electrolysers. Kick-off meeting for the IEA Technology Roadmap on Hydrogen; 2013 Jul 9-10; Paris, France. Available from https://www.iea.org/media/workshops/2013/hydrogenroadmap/Session4.2WaidhasSiemens.pdf.

[9] Department of Energy (DOE). Solar and Wind Technologies for Hydrogen Production. Report to Congress; 2005 Dec. No.:ESECS EE-3060.

[10] Levene JI. Economic Analysis of Hydrogen Production from Wind. Golden (CO): National Renewable Energy Laboratory; 2005 May. Report No.: NREL/CP-560-38210.

[11] Amos WA. Costs of Storing and Transporting Hydrogen. Golden (CO): National Renewable Energy Laboratory; 1998 Nov. Report No.: NREL/TP-570-25106.

[12] Steward D, Saur G, Penev M, Ramsden T. Lifecycle Cost Analysis of Hydrogen Versus Other Technologies for Electrical Energy Storage. Golden (CO): National Renewable Energy Laboratory; 2009 Nov. Report No.: NREL/TP-560-46719.

[13] Schoenung S. Hydrogen Energy Storage Comparison. 1999 Mar. Report No.: DE-FC36-96-GOI 0140. A003. Prepared for United States Department of Energy.

[14] Schoenung S. Economic Analysis of Large-Scale Hydrogen Storage for Renewable Utility Applications. Albuquerque (NM): Sandia National Laboratories; 2011 Aug. Report No.: SAND2011-4845.

[15] Zhou Z, Maeda T, Ishida M. Capacity Planning and Economical Evaluation of a Renewable Power System for Remote Island. IEEJ Transaction PE 2013;133(1):19-25. DOI: 10.1541/ieejpes.133.19. (in Japanese)

[16] Kroposki J, Levene K, Harrison PK, Sen FN. Electrolysis: Information and Opportunities for Electric Power Utilities. Golden (CO): National Renewable Energy Laboratory; 2006 Sep. Report No.: NREL/TP-581-40605.

[17] Harrison KW, Martin GD, Ramsden TG, Kramer WE, Novachek FJ. The Wind-to-Hydrogen Project: Operational Experience Testing, and Systems Integration. Golden (CO): National Renewable Energy Laboratory; 2009 Mar. Report No.: NREL/TP-550-44082.

[18] Saur G, Ramsden T. Wind Electrolysis: Hydrogen Cost Optimization. Golden (CO): National Renewable Energy Laboratory; 2011 May. Report No.: NREL/TP-5600-50408.

[19] Schaber K., Steinke F, Hamacher T. Transmission grid extensions for the integration of variable renewable energies in Europe: Who benefits where ?. Energy Policy 2012;43:123–135. DOI: 10.1016/j.enpol.2011.12.040.
Available from http://dx.doi.org/10.1016/j.enpol.2011.12.040.

[20] Komiyama R, Fujii Y. Assessment of massive integration of photovoltaic system considering rechargeable battery in Japan with high time-resolution optimal power generation mix model. *Energy Policy* 2014;66:73-89. DOI: 10.1016/j.enpol.2013.11.022.
Available from http://dx.doi.org/10.1016/j.enpol.2013.11.022.

[21] Komiyama R, Fujii Y. Energy modeling and analysis for optimal grid integration of large-scale variable renewables using hydrogen storage in Japan. *Energy* 2015. DOI: 10.1016/j.energy.2014.12.069. Available from http://www.sciencedirect.com/science/article/pii/S0360544214014492.

[22] Komiyama R, Shibata S, Nakamura Y, Fujii Y. Analysis of possible introduction of PV systems considering output power fluctuations and battery technology, employing an optimal power generation mix model. Elect. Eng. Jpn., Wiley. 2012;182(2):9-19. DOI: 10.1002/eej.22329. Available from http://onlinelibrary.wiley.com/doi/10.1002/eej.22329/abstract.

[23] Komiyama R, Shibata S, Fujii Y. Simulation Analysis for Massive Deployment of Variable Renewables employing an Optimal Power Generation Mix Model. Journal of Energy and Power Engineering 2013;7: 1604-1615.

[24] Komiyama R, Fujii Y. Assessment of Japan's Optimal Power Generation Mix Considering Massive Deployment of Variable Renewable Power Generation. Elect. Eng. Jpn.. Wiley. 2013;185: 1–11. DOI: 10.1002/eej.22470.
Available from http://onlinelibrary.wiley.com/doi/10.1002/eej.22470/abstract.

[25] Hashimoto T, Kurita A, Minami M, Yoshioka M, Kobayashi K, Hashimoto M. Development of Grid-stabilization Power-storage Systems Using Lithium-ion Rechargeable Batteries. Mitsubishi Heavy Industries Technical Review. 2011;48(3):48-55.

[26] Hida Y, Yokoyama R, Shimizukawa J, Iba K, Tanaka K, Seki T. Load following operation of NAS battery by setting statistic margins to avoid risks. IEEE PES General Meeting 2010; 2010 Jul 25-29; Minneapolis, MN.
Available from http://ieeexplore.ieee.org/stamp/stamp.jsp?arnumber=5588170.

[27] K+S Group. Global Salt Deposits; [cited 2013 Oct 3].
Available from http://www.k-plus-s.com/en/wissen/rohstoffe/salzvorkommen.html.

[28] Ministry of the Environment in Japan. Study of Basic Zoning Information Concerning Renewable Energies (FY2011). 2012 Jun. (in Japanese)
English summary is available from http://www.env.go.jp/earth/report/h24-04/summary_en.pdf.

[29] Komiyama R, Fujii Y. Optimal Power Generation Mix considering Hydrogen Storage of Variable

Renewable Power Generation. In Japanese, IEEJ Transaction PE.2014;134(10), 885-89.

[30] Eckroad S. Vanadium Redox Flow Batteries: An In-Depth Analysis. Palo Alto (CA): Electric Power Research Institute; 2007 Mar. Report No.:1014836.

[31] Rastler D. Electricity Energy Storage Technology Options: A White Paper Primer on Applications, Costs and Benefits. Palo Alto (CA): Electric Power Research Institute; 2010 Dec. Report No.:1020676.

[32] Ministry of Economy, Trading and Industry, Japan (METI). Establishment of Low Carbon Electric Power Supply System. METI; 2009 Jul. (in Japanese)
Available from http://www.meti.go.jp/report/downloadfiles/g90727e03j.pdf.

[33] Ministry of Economy, Trading and Industry, Japan (METI). Future of Battery Industry in Japan. METI; 2010 May. (in Japanese)
Available from http://www.meti.go.jp/report/downloadfiles/g100519a02j.pdf.

[34] Japan Meteorological Agency, Japan (JMA). Automated Meteorological Data Acquisition System (AMeDAS). JMA; 2007. (in Japanese)

[35] Schoenung S. Energy Storage Systems Cost Update. Albuquerque (NM): Sandia National Laboratories; 2011 Apr. Report No.: SAND2011-2730.